Proceedings of Ninth World Conference on Earthquake Engineering
August 2-9, 1988, Tokyo-Kyoto, JAPAN (Vol.III)

5-3-1

BASIC STUDY ON THE DYNAMIC BEHAVIOR OF SOIL-PILE INTERACTION ANALYSIS OF A LATERALLY LOADED PILE

Kaeko YAHATA[1] and Osamu MATSUOKA[2]

[1]Kajima Institute of Construction Technology, Chofu-shi, Tokyo, Japan
[2]Department of Technology, Nagoya University, Chigusa-ku, Nagoya, Japan

SUMMARY

This paper investigates the dynamic behavior of two kinds of soil-pile system which are a floating pile in a half-space and a supporting pile in a surface layer on a rigid bed rock by an analytical method. As two kinds of rigorous solution obtained from three dimensional elastic wave-propagation theory are applied to solve soil-pile interaction, soil dynamics is sufficiently estimated. Significant properties of depending upon the different conditions of the pile tip in the different elastic solids are clarified. The validity of the method is discussed in the comparison with a similar previous static study.

INTRODUCTION

It is the purpose of this paper to investigate the basic dynamic behavior of soil-pile interaction by the analytical method presented by the authors.[1] The complete solutions described below are applied in this method to solve soil-pile interaction problem. These solutions are to the problem of an elastic solid subjected to a harmonic point load in its interior and were obtained by three dimensional elastic wave-propagation theory in a homogeneous, isotropic medium as discussed by the authors. The solutions were obtained for two kinds of elastic solid :a half-space and a surface layer on a rigid bed rock. Those are regarded as Green's function satisfying the boundary conditions for each type of solid. This study is an extension of the well known static soil-pile analysis by Poulos[2] to dynamic analysis, and clarifies the properties of a laterally loaded pile in taking into account the different responses resulting from two solutions. The studies by Poulos have greatly contributed to the dynamic pile investigations in the evaluation of the results. This paper discusses a comparison of the basic responses of a floating pile in a half space and a supporting pile in the surface layer. Novak and Nogami[4] presented the dynamic analysis of soil-pile interaction for the first time based on continuum analysis. Considering the great developments in soil-foundation problem using Lamb's solution, it should be possible to effectively solve soil-pile interaction in similar manner using the solution of a harmonic point load in order to properly estimate the effect of soil radiation damping.

THE COMPLETE SOLUTION OF A HARMONIC POINT LOAD IN AN ELASTIC SOLID

Firstly, two kinds of complete solution are presented because studies on their properties are available for the prospect of the responses of soil-pile

interaction. The following two equations are the solutions for a half-space and the surface layer. The lateral displacement in a half-space subjected to a laterally harmonic point load without material damping is eq. (1).

$$U_1 = \frac{X_1'}{4\pi G} e^{i\omega t} \frac{1}{\beta_1^2} \int_0^\infty \frac{-s\sigma_{33}'\{(2\xi^2-\beta_1^2)\, e^{-\gamma_1 z} - 2\gamma_1\gamma_2 e^{-\gamma_2 z}\}}{\gamma_1\{(2\xi^2-\beta_1^2)^2 - 4\gamma_1\gamma_2\xi^2\}} \xi^3 \cdot \{-J_0(r\xi) + (\frac{2x^2}{r^2}-1) J_2(r\xi)\}\, d\xi + \frac{X_1'}{4\pi G} e^{i\omega t} [\frac{1}{R_1} e^{-i\beta_1 R_1} + \frac{1}{R_2} e^{-i\beta_1 R_2} + \frac{1}{\beta_1^2}\{\frac{1}{R_1}(e^{-i\beta_1 R_1} - e^{-i\beta_1 R_1}) + \frac{1}{R_2}(e^{-i\beta_1 R_2} - e^{-i\beta_1 R_2})\}] \quad (1)$$

$$R_1 = \sqrt{x^2+y^2+(z-c)^2},\quad R_2 = \sqrt{x^2+y^2+(z+c)^2} \qquad r = \sqrt{x^2+y^2}$$

$$s\sigma_{33}' = (-2\xi^2+\beta_1^2)\, e^{-c\gamma} + 2\gamma_1\gamma_2 e^{-c\gamma_2} \qquad \gamma_1 = \sqrt{\xi^2-\beta_1^2},\ \gamma_2 = \sqrt{\xi^2-\beta_1^2},\ \xi^2 = k_1^2 + k_1^2$$

where X_1': Amplitude of a point load; G: Shear modulus of soil; c: Acting position of a point load; C_1, C_2: Velocity of longitudinal and transverse waves, respectively, and $\beta_1=\omega/C_1$, $\beta_2=\omega/C_2$; x, y, z: Adopted orthogonal Cartesian coordinates; k_1, k_2: Variables after Fourier transform of x, y coordinates.

This solution coincides with Mindlin[5] solution when frequency approaches zero. A similar solution for the surface layer is eq.(2).

$$U_1 = \frac{X_1'}{4\pi G} e^{i\omega t} \frac{1}{\beta_1^2} [\int_0^\infty \frac{1}{F(\xi)}\{(A_1' e^{-\gamma_1 z} + A_2' e^{\gamma_1 z}) + \gamma_2 (D_1' e^{-\gamma_2 z} - D_2' e^{\gamma_2 z})\} - \frac{1}{2}(B_1' e^{-\gamma_2 z} + B_2' e^{\gamma_2 z})] \xi^3 \{-J_0(r\xi) + (\frac{2x^2}{r^2}-1) J_2(r\xi)\}\, d\xi - \frac{\beta_2^2}{2}\int_0^\infty (B_1' e^{-\gamma_2 z} + B_2' e^{\gamma_2 z}) \xi J_0(r\xi)\, d\xi + \beta_2^2 (\frac{e^{-i\beta_2 R_1}}{R_1} + \frac{e^{-i\beta_2 R_2}}{R_2}) + \frac{\partial^2}{\partial x^2}\{\frac{1}{R_1}(e^{-i\beta_2 R_1} - e^{-i\beta_1 R_1}) + \frac{1}{R_2}(e^{-i\beta_2 R_2} - e^{-i\beta_1 R_2})\}] \quad (2)$$

$$A_1' = \frac{X_1'}{2G\beta_2^2} e^{i\omega t} \frac{1}{F(\xi)} [P_1\{-2\xi^2 f_2 + e^{(\gamma_1-\gamma_2)H} \cdot f_1(\frac{f_2}{2}+\xi^2) + e^{(\gamma_1+\gamma_2)H} f_1(\frac{f_2}{2}-\xi^2)\} + P_2\{e^{-\gamma_2 H}\xi^2(2f_2\xi^2 - f_1^2) + e^{\gamma_2 H}\xi^2(2f_2\xi^2+f_1^2) - e^{\gamma_1 H}(2f_1 f_2 \xi^2)\} + P_3\{e^{-\gamma_2 H}\gamma_1(2f_2\xi^2 - f_1^2) - e^{\gamma_2 H}\gamma_1(2f_2\xi^2+f_1^2) + e^{\gamma_1 H}\gamma_1(4f_1\xi^2)\}]$$

$$A_2' = \frac{X_1'}{2G\beta_2^2} e^{i\omega t} \frac{1}{F(\xi)} [P_1\{-2\xi^2 f_2 + e^{-(\gamma_1-\gamma_2)H} \cdot f_1(\frac{f_2}{2}+\xi^2) + e^{-(\gamma_1+\gamma_2)H} f_1(\frac{f_2}{2}-\xi^2)\} + P_2\{e^{\gamma_2 H}\xi^2(2f_2\xi^2 - f_1^2) + e^{\gamma_2 H}\xi^2(2f_2\xi^2 - f_1^2) - e^{-\gamma_1 H}(2f_1 f_2 \xi^2)\} + P_3\{-e^{-\gamma_2 H}\gamma_1(2f_2\xi^2 - f_1^2) + e^{-\gamma_2 H}\gamma_1(2f_2\xi^2+f_1^2) - e^{-\gamma_1 H}\gamma_1(4f_1\xi^2)\}]$$

$$D_1' = \frac{X_1'}{2G\beta_2^2} e^{i\omega t} \frac{1}{F(\xi)} [P_1 \cdot 2\gamma_1\{-f_1 + e^{-(\gamma_1-\gamma_2)H} \cdot (\frac{f_2}{2}+\xi^2) - e^{(\gamma_1+\gamma_2)H}(\frac{f_2}{2}-\xi^2)\} + P_2 \cdot 2\gamma_1\{-\frac{e^{-\gamma_1 H}}{2}(2f_2\xi^2 - f_1^2) + \frac{e^{\gamma_1 H}}{2}(2f_2\xi^2+f_1^2) - e^{\gamma_2 H}(2f_2\xi^2)\} + P_3\{-e^{\gamma_1 H}(2f_2\xi^2 - f_1^2) - e^{\gamma_1 H}(2f_2\xi^2+f_1^2) + e^{\gamma_2 H}(2f_1 f_2)\}]$$

$$D_2' = \frac{X_1'}{2G\beta_2^2} e^{i\omega t} \frac{1}{F(\xi)} [P_1 \cdot 2\gamma_1\{f_1 - e^{(\gamma_1-\gamma_2)H} \cdot (\frac{f_2}{2}+\xi^2) + e^{-(\gamma_1+\gamma_2)H}(\frac{f_2}{2}-\xi^2)\} + P_2 \cdot 2\gamma_1\{\frac{e^{\gamma_1 H}}{2}(2f_2\xi^2 - f_1^2) - \frac{e^{\gamma_1 H}}{2}(2f_2\xi^2+f_1^2) + e^{-\gamma_2 H}(2f_2\xi^2)\} + P_3\{-e^{\gamma_1 H}(2f_2\xi^2+f_1^2) - e^{-\gamma_1 H}(2f_2\xi^2 - f_1^2) + e^{-\gamma_2 H}(2f_1 f_2)\}]$$

$$s_0\sigma_{33} = -\frac{2}{\gamma_2}\{(-2\xi^2+\beta_2^2) e^{-c\gamma_2} + 2\gamma_1\gamma_2 e^{-c\gamma_2}\} \quad {}_{SH}U_2 = -\{\frac{1}{\gamma_2}(e^{-\gamma_2|2H-c|} + e^{-\gamma_2|2H+c|}) - \frac{1}{\gamma_1}(e^{-\gamma_1|2H-c|} + e^{-\gamma_1|2H+c|})\} \quad {}_{SH}U_3 = -(-e^{-\gamma_2|2H-c|} - e^{-\gamma_2|2H+c|} + e^{-\gamma_1|2H-c|} + e^{-\gamma_1|2H+c|})$$

$$P_1 = 4\gamma_2^2 B_1' + s_0\sigma_{33}.\quad P_2 = {}_{SH}U_2 + (e^{-\gamma_2 H} + e^{\gamma_2 H}) B_1',\quad P_3 = {}_{SH}U_3 - \gamma_2 (e^{-\gamma_2 H} - e^{\gamma_2 H}) B_1'$$

$$f_1 = 2\xi^2 - \beta_2^2.\quad f_2 = 2\gamma_1\gamma_2 \qquad B_1' = B_2' = (X_1'/2G\beta_2^2) e^{i\omega t}\{e^{-\gamma_2 H}\cosh(\gamma_2 c)/\gamma_2\cosh(\gamma_2 H)\}$$

$$\det(aij) = \frac{1}{2\gamma_1}[-16\gamma_1\gamma_2(2\xi^2-\beta_2^2)\xi^2 + 2\{(2\xi^2-\beta_2^2)^2 - 4\gamma_1\gamma_2\xi^2\}(\gamma_1\gamma_2 - \xi^2)\cosh\{(\gamma_1+\gamma_2)H\} + 2\{(2\xi^2-\beta_2^2)^2 + 4\gamma_1\gamma_2\xi^2\}(\gamma_1\gamma_2+\xi^2)\cdot\cosh\{(\gamma_1-\gamma_2)H\}] = \frac{1}{2\gamma_1} F(\xi)$$

where H: Surface layer thickness.

The solution coincides with eq. (1) if the surface layer thickness is infinite. The denominator in the first term of eq.(1) is Rayleigh function of a half-space, and $F(\xi)$ in eq. (2) is that of the surface-layer. The solutions of

eqs. (1) and (2) are determined by carrying out complex numerical integration. The solutions consist of three parts: fundamental solution, potential function satisfying the boundary conditions derived from the Helmholtz decomposition theorem, and the residues. Numerical integration is necessary to obtain Cauchy principal value in inverse Fourier transformation. As the range of integration includes singular points, their positions should be obtained from Rayleigh and Love functions before integration despite the troublesome procedure .

The displacements (U_1) at the origin (0, 0, 0) on the free surface under a lateral harmonic point load acting at $\beta_2 H/\beta_2 c=0.5$ are plotted in Fig. 1. Poisson's ratio (ν) for each elastic solid is taken to be 1/3. As the expressions are nondimensional, displacements with dimension are obtained after multiplying them by the coefficient ($X_1 \beta_2 e^{i\omega t}/4\pi G$). The response displacements in Fig. 1 are the results of the varying load position from about 0 to 3.5, so in other words, $\beta_2 c$ is located in the middle of the surface layer. The displacements of the two solutions change with moving $\beta_2 c$, and the general tendencies in both responses are similar. However the characteristics of the surface layer are different from those of a half-space because of the strong influence of the resonance frequencies. Both sets of results become gradually closer with increasing frequency except close to the resonance frequency. In order to clarify the influence of the boundary condition at the bottom of the surface layer, the deflection curves resulting from changing the applied load position by equal intervals of 0.4 for the surface thickness $\beta_2 H=4.0$ are shown in Fig. 2. The differences between the responses increase with increasing depth of the applied load, especially in the imaginary part. As there are resonance frequencies in the surface layer, the dynamic response in this case exhibits more complex features than for a half-space. The movement of the load has much effect on the response and this tendency is closely related to soil-pile interaction responses.

ANALYSIS OF SOIL-PILE INTERACTION

The procedure employed here is similar to the method presented by Poulos, except that dynamic solutions are given. Two types of soil-pile system are analyzed to compare the influence of different conditions of the pile tips in different elastic solids. These consist of a floating pile in a half-space, case(a), and a supporting pile in the surface layer, case(b). A laterally harmonic load ($Qe^{i\omega t}$) acts at the pile head. The method is only briefly described below because full details are given in the reference. The pile is assumed to be a thin vertical strip corresponding to the center of the cross section, and the interface between the soil and the strip is assumed to have a perfect contact. L and d denote the length and width of a pile, respectively. The pile is divided into n+1 elements in order to apply finite-difference method to the governing equation for lateral motion of the pile. The centers of all elements except those at both ends satisfy the displacement equilibrium, including boundary conditions. Distributed pressures are assumed to be uniform on each element.

The governing equation is

$$m_p \frac{\partial^2}{\partial t^2} ({}_pU_1 e^{i\omega t}) + E_p I_p \frac{\partial^4}{\partial z^4} ({}_pU_1 e^{i\omega t}) = P(z) e^{i\omega t} \qquad (3)$$

where ${}_pU_1$: Lateral displacement of the pile; Mp: Mass density per unit length of the pile; EpIp: Flexural rigidity of the pile; P(z): Amplitude of the force of resistance of the soil.

Boundary conditions at the fixed head (z=0) for both cases are $EpIp(d^3 {}_pU_1/dz^3)=Qe$; $EpIp(d {}_pU_1/dz)=0$. Boundary conditions at the pile tip (z=L) for a floating pile are free. So these are $EpIp(d^2 {}_pU_1/dz^2)=0$; $EpIp(d^3 {}_pU_1/dz^3)=0$. The

boundary conditions of it for a supporting pile are fixed. So these are $_pU_1=0$; $EpIp(d\ _pU_1/dz)=0$; The relation between the soil displacement and the pile load can be represented by the following matrix for the discrete system of the dividing elements. That is $\{_sU_1\}=[F]\{P'\}$: Where[F]is displacement function matrix obtained by integrating the solution of a hamonic point load in the interior of each solid across the element area of the strip,$\{P'\}$is amplitude matrix of the pile load, and$\{_sU_1\}$ is lateral displacement matrix of the soil at the center of each element except both end elements or at the points of both end elements.

After expressions of discrete system for eq. (3), $\{P\}$;$\{_pU_1\}$ should be equal to $-\{P'\}$;$\{_sU_1\}$in the matrix, and then either displacement or resistance force is determined. Considering the discussion in Fig. 1, studies are conducted to obtain the different properties of two kinds of soil-pile system with physical parameters $Mp=(2.4\ t/m^2)\cdot$ section area/$(9.8\ m/sec^2)$; L=4m; slenderness ratio d/L=0.1;and β_2L=2.0, 3.0, 4.7, 6.0. These cases are designated case(a)-2.0, case(a) -3.0, ...case(b)-6.0. Fig. 3 indicates each displacement function for the 11 elements. The real parts of case(a) show a similar tendency to those of case(b). However, as the load approaches deeper positions near the fixed end, the difference increases. The displacement in case(b)-4.7 appears to be influenced by the second shear mode of the surface layer. As for the imaginary parts, differences between cases(a) and (b) occur when the load acts at deeper positions. The response tendency depends upon the value of β_2H. Thus, the discrepacy between case(b)-4.7 and case(a)-4.7 is large, but it is small for the cases when β_2H=6.0 even though the depth of the applied load is greater. The displacement with dimension can be obtained after multiplying the amplitude in Fig. 3 by $x'e^{i\omega t}/(4\pi G\beta_2)$, where x' is the amplitude of the uniform pressure acting on each element. Compared with the real parts, the properties of the imaginary parts are characteristic because there are large differences between both cases with the load applied at deep positions.

The variations of the pile displacements for the pile flexibility factor $K_R=EpIp/EsL^4$, where Es is Young's modulus, which corresponds to relative relations between the soil and pile are plotted in Fig. 4. K_R is given the four values 10^{-4},10^{-3},10^{-2},and 10^{-1}. The displacement with dimension per unit load is obtained after multiplying the amplitude in Fig. 4 by$(e^{i\omega t}/4\pi G\beta_2)$. While the imaginary parts don't depend upon K_R for small values of β_2L such as 2.0 and 3.0, they do vary with K_R for relatively large values such as 4.7 and 6.0. Special features are observed for $K_R=10^{-1}$ because it strongly reflects the fixed end condition. As K_R becomes small, the discrepacy between cases (a) and (b) decreases because the influence of shallow applied loads is greater and that of deep loads is less. It can be imagined that the opposite phenomenon occurs for large K_R. Although case(b)-3.0 and case(b)-4.7 are located at similar points near the resonance frequency, and the response in case(b)-4.7 is siginificantly influenced by this fact, the same cannot be observed in case(b)-3.0 especially in the imaginary part. One reason for the different properties is that the resonance frequency in case(b)-4.7 comes from the double poles in Love function, and it corresponds to Rayleigh function for case(a)-3.0. As for the case of β_2L=6.0, the difference between cases (a) and (b) is slight because the influence of the resonance frequency is small and it exists at a relatively high frequency.

Fig. 5 shows influence factors (IpF) defined as $pU_1=IpF\ Qe^{i\omega t}/(Es\ L)$at the pile head. IpF corresponds to impedance in soil-pile interaction. It can be seen that the differences between cases(a) and (b) arise when K_R is greater than 10^{-2}. This observation agrees with Poulos[3] study. The effective contribution of the different conditions is reflected more sensitively in the imaginary part than the real part. The response in the real part depends very much upon K_R greater than 10^{-3}, whatever the value of β_2L. On the other hand, the range of the dependence on K_R in the imaginary part varies with β_2L.

COMPARISON WITH OTHER SOLUTION AND CONCLUSION

The dynamic responses of short and long piles of the floating type in a half-space are obtained in order to make a comparison with Poulos' solution. The physical parameters used are L/d =10 and 100 for short and long piles, respectively with ν=0.4. The displacement amplitudes of the resonance curves at three positions of the pile (pile head, 0.2L from the head and pile tip) are shown in Fig. 6 for $K_R=10^{-4}$, 10^{-5}, 10^{-6}. The displacement with dimension is obtained after carrying out similar manner for the amplitude in Fig. 6 to case of Fig. 4. The responses of the long pile depend very much upon frequency and K_R in any position. However the tendency of dependence on K_R is different for each point. On the other hand, the dependence on frequency is small for the short pile because it is affected less by the dynamic behavior of the soil than the long pile. It may be significant for pile behaviors to pay much attention to the properties at deep positions. A comparison is made in Fig. 7 with Poulos' result for v=0.5 . The present solution is sufficiently close to it after taking into account the slight differences of low frequency(0.5Hz) and Poisson's ratio of 0.4 are adopted in the analysis.

In conclusion, the different behaviors of two types of soil-pile system are analyzed using two kinds of complete solution. Special features of the surface layer due to the resonance frequency affect the responses of depending upon K_R for soil-pile interaction.

As the present method has been verified and the procedure is general, there is much possibility of being able to extend the method to soil-pile group interaction.

REFERENCES

1. Matsuoka, O. and Yahata, K., "Basic Analyses on Problems of a Three Dimensional Homogeneous, Isotropic, Elastic Medium, and the Applications," Part(I)-Part(V), Tran. Architec. Inst. Japan, No.288(1980), No.293(1980), No.298(1980), No.330(1983), No.347(1985).
2. Poulos, H.G., "Behaviour of Latterally Loaded Piles: I-Single Piles," ASCE 97, SM5, (1971)
3. Poulos, H.G., "Behaviour of Latterally Loadeda Piles: III-Socketed Piles," ASCE 98, SM4, (1972)
4. Nogami, T. and Novak, Mo, "Resistance of Soil to a Horizontally Vibrating Pile," Earth. Eng. Struct. Dyn. 5 (1977)
5. Mindlin, R.D., "Force at a Point in the Interior of a Semi-Infinite Solid," Physics 7 (1936)

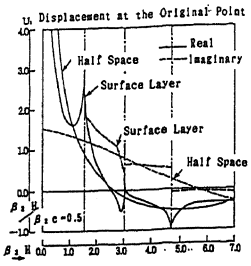

Fig.1 Surface Responses on Loaded Point at the Center of the Surface Layer Depth

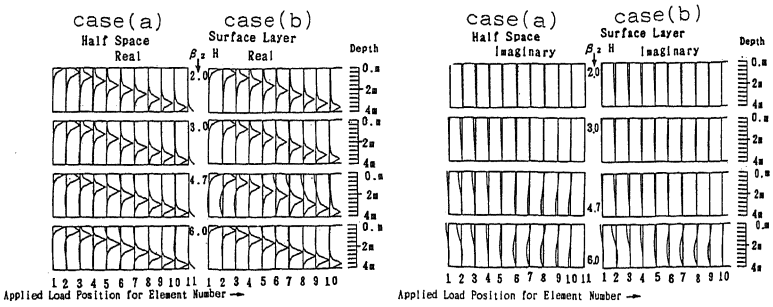

Fig.3 Displacement Function

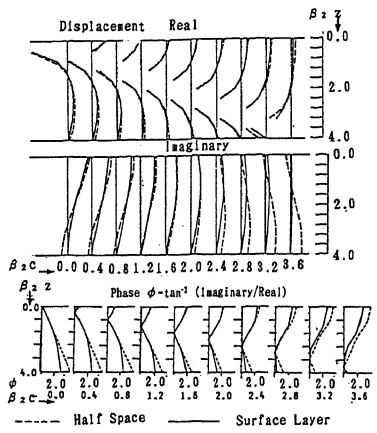

Fig.2 Responses with Varying Loaded Point

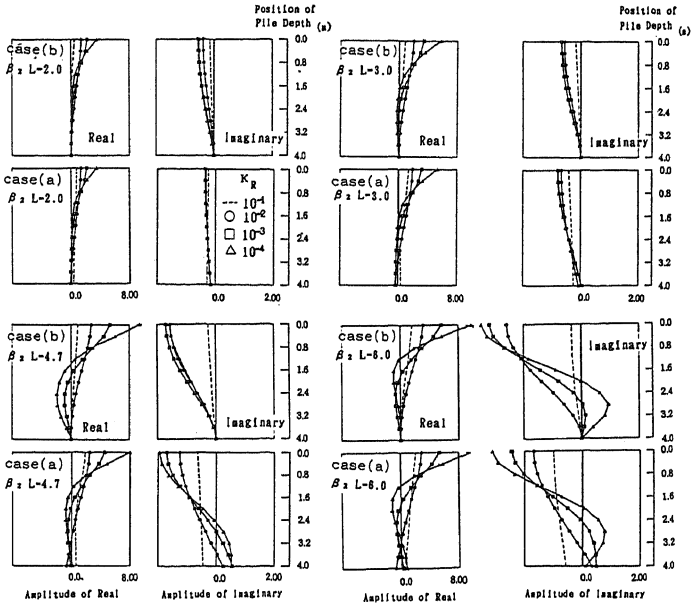

Fig.4 Deflection Curves with Pile Flexibility Factor

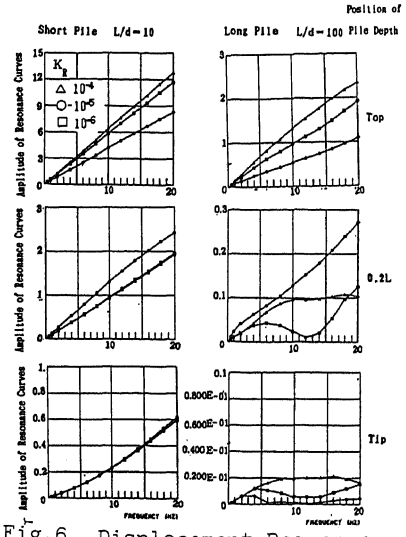

Fig.6 Displacement Responses on Variable Position of Pile

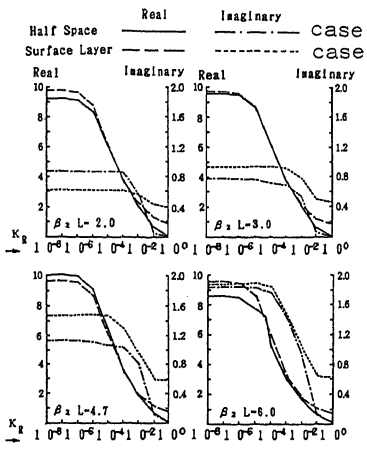

Fig.5 Influence Factors of a Pile Head with Flexibility Factor

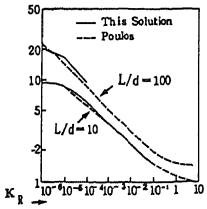

Fig.7 Comparison of Influence Factor